

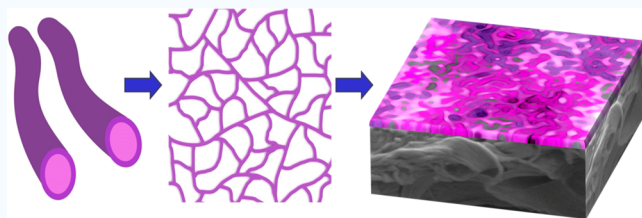
High Flux Membranes with Ultrathin Zwitterionic Copolymer Selective Layers with \sim 1 nm Pores Using an Ionic Liquid Cosolvent

Prity Bengani-Lutz, Ilin Sadeghi,^{ID} Samuel J. Lounder, Matthew J. Panzer,^{ID} and Ayse Asatekin*^{ID}

Department of Chemical and Biological Engineering, Tufts University, 4 Colby Street, Medford, Massachusetts 02155, United States

Supporting Information

ABSTRACT: We report membranes with ultrathin <200 nm zwitterionic copolymer selective layers exhibiting \sim 1 nm size cutoff and permeances as high as 50 L/m²·hr·bar. The thin layer is formed by the deposition of random zwitterionic copolymers in trifluoroethanol/ionic liquid mixtures onto a porous support. The resultant membranes have the same low molecular weight cutoff of \sim 1000 Da and narrow pore size distribution but fluxes up to 10 times higher than membranes prepared without ionic liquid and 20 times higher than commercial membranes of similar pore size, making them promising for wastewater treatment and pharmaceutical purification.



KEYWORDS: zwitterion, membrane, ionic liquid, sulfobetaine, self-assembly

Membranes are a crucial technology for water and wastewater treatment, bioseparations, and chemical manufacturing. Most commercial membranes today are manufactured from a handful of commodity polymers, relying on the complex interplay of phase separation and transport that occurs during the manufacturing process. Recently, polymer self-assembly has gained traction as a crucial tool for scalable manufacture of next generation membranes with desired properties such as high permeability and controlled pore size.^{1–3} For example, the self-assembly of block copolymers (BCPs) into well-defined nanostructures has been used to create isoporous ultrafiltration (UF) membranes using self-assembly nonsolvent induced phase separation (SNIPS).^{4–8} Alternatively, random and graft copolymers have been used as membrane selective layers to achieve smaller pore sizes down to \sim 1 nm and simplify synthesis methodologies.^{9–13}

Recently, we reported the use of amphiphilic random zwitterionic copolymers (RZCs) as membrane selective layers for size-based separation of small molecules.^{11–13} These membranes take advantage of the incompatibility between the hydrophobic (2,2,2-trifluoroethyl methacrylate (TFEMA)) and hydrophilic zwitterionic repeat units (sulfobetaine methacrylate (SBMA)) and the ability of zwitterions to self-assemble in a broad range of conditions through strong electrostatic interactions.^{11–15} These RZCs self-assemble into bicontinuous networks of hydrophobic and zwitterionic domains \sim 1 nm in size. The zwitterionic domains act as a network of nanochannels through which water and solutes pass, creating highly permeable membrane selective layers with a \sim 1 nm size cutoff. This corresponds to a molecular weight cutoff (MWCO) of \sim 1000 Da, a valuable pore size for difficult bioseparations and wastewater treatment applications.^{11–13,16}

These membranes are also extremely fouling resistant, further expanding their promise.

In previous studies, we prepared these membranes by coating a solution of the RZC in trifluoroethanol (TFE) onto a commercial ultrafiltration (UF) membrane, creating thin film composite (TFC) membranes with \sim 1 μ m thick selective layers. Membrane permeances ranged between 1.4 and 8 L/m²·hr·bar, comparable to or higher than a commercial membrane with similar nominal MWCO.^{10,11} Most commercial TFC membranes, however, have much thinner selective layers, usually between 20 and 200 nm in thickness.¹⁷ Creating such ultrathin selective layers by coating copolymer solutions is challenging. Taking advantage of polymer self-assembly in solution may enable interesting selective layer morphologies⁹ and/or thinner selective layers. Zwitterionic amphiphiles self-assemble in various solvents, especially in water or solvent mixtures that contain water.^{18,19} In nonaqueous organic solvents, micelle formation is typically mediated by the presence of salts.²⁰ RZCs can in principle form micelles in solution, but the close proximity of incompatible repeat units in random copolymers makes this less likely. While one study reported round micelles in aqueous solutions of an RZC with phosphorylcholine groups,²¹ there are no studies that report the supramolecular assembly of RZCs in organic solutions.

Ionic liquids (ILs) are molten salts at room temperature. Their negligible vapor pressures, high chemical stability, and wide electrochemical windows have led to their use in a variety of applications such as energy storage devices and catalysis.²² Due to their high polarities, strong interactions are predicted between ILs and zwitterionic groups.^{18,23–27} ILs can

Received: April 30, 2019

Accepted: June 28, 2019

Published: June 28, 2019

Table 1. Coating Solution Composition for Membranes Used in This Study

membrane code	coating solution composition			water permeance (L/m ² ·hr·bar)	selective layer thickness (μm)
	copolymer (g)	TFE (mL)	EAN (mL)		
P0	1	9.0	0	6.1 ± 1	1 ± 0.1
IL2	1	8.8	0.2	0.7 ± 0.2	1.1 ± 0.1
IL5	1	8.5	0.5	1.7 ± 0.7	0.7 ± 0.1
IL20	1	7.0	2.0	50 ± 2	<0.2

solubilize hard to dissolve zwitterionic materials²³ and alter the size and properties of zwitterionic surfactant micelles in water.²⁴ In turn, zwitterions can enhance the dissociation of ILs, leading to enhanced ionic conductivity.^{25,26} Zwitterionic BCPs can form polymersomes in ILs,²⁷ indicating the possibility of IL mediated micelle formation.

In this work, we examined the potential of an IL as a cosolvent for random zwitterionic copolymers (RZC) to prepare ultrathin membrane selective layers to achieve membranes with size-based selectivity, ~1 nm effective pore size, yet very high permeance. We show that when the RZC is dissolved in IL/TFE mixtures and coated onto a porous substrate, very thin (<200 nm) selective layers can be obtained. This leads to permeances as high as 50 L/m²·hr·bar, up to 10 times higher than membranes formed without IL cosolvent. These membranes also exhibit a narrow pore size distribution, retaining the same size-based selectivity with a ~1 nm size cutoff. This enhancement in permeance depends on the amount of IL and the manufacturing method (nonsolvent, drying time etc.). We hypothesize that the formation of these very thin layers is likely enabled by the formation of supramolecular assemblies upon partial evaporation of TFE, followed by their deposition onto the surface of the porous support. These new membranes with high permeances and sharp selectivity are promising for various applications such as textile wastewater treatment and pharmaceutical purification.

This study focused on membranes whose selective layers were made of the RZC poly(trifluoroethyl methacrylate-random-sulfobetaine methacrylate) (PTFEMA-*r*-SBMA), synthesized by free radical copolymerization.^{11–13} The copolymer contained 36 wt % SBMA with a relative molecular weight of 1.19×10^6 g/mol based on polyacrylonitrile standards in dimethylformamide (see Supporting Information). This copolymer is soluble in TFE and dimethyl sulfoxide and insoluble in water. Ethylammonium nitrate (EAN, Iolitec) was selected as the IL cosolvent due to its miscibility with TFE and water. TFE is volatile (boiling point ~78 °C), whereas EAN has low volatility (boiling point ~200 °C²⁸). PSBMA and PTFEMA homopolymers and the RZC were all soluble in TFE. PTFEMA and the RZC were insoluble in EAN, while PSBMA dissolved in it readily, indicating that this IL is a selective solvent for the zwitterionic repeat units.

Membranes were prepared by dissolving the RZC in EAN:TFE:RZC mixtures at various ratios from 0:90:10 to 20:70:10 (Table 1). The copolymer concentration was kept constant at 10% (w/v). Solutions were prepared by first blending the solvents and then dissolving the copolymer at 50 °C, passing the solution through a 0.45 μm syringe filter (Whatman), and degassing it in a vacuum oven. The copolymer solution was coated on a commercial polyvinylidene-fluoride (PVDF) 400R UF membrane (Nanostone Water) using a doctor blade with a 25 μm gap. The membrane was then immersed in an isopropanol bath for 20 min to precipitate out the copolymer, moved to a water bath at least overnight,

and then stored in a fresh water bath until use. The IL is expected to be removed in the water bath.

Filtration experiments were performed on 25 mm diameter membranes using a 10 mL Amicon 8010 stirred, dead-end filtration cell (Millipore, effective filtration area 4.1 cm²). Water flow rate through the membranes was measured at a trans-membrane pressure (TMP) of 20 psi (1.4 bar). Membrane permeance was calculated by dividing the flow rate by the membrane area and TMP. Membrane selectivity was quantified by measuring the rejections of charged and neutral solutes in filtration experiments. This method utilizes rigid water-soluble organic molecules as probes for characterizing effective pore size. Molecular diameters were calculated by determining the molecular volume of the solute and calculating the diameter of a sphere of equivalent volume, following previous publications.^{11,12,29–31}

The addition of small amounts of IL to the coating solution led to slight decreases in water permeance (Table 1, Figure 1a). However, when the coating solution contained 20% IL (sample IL20), the water permeance rose to approximately 10 times that of P0 membranes prepared without IL. This drastic increase in flux was not accompanied by any changes in

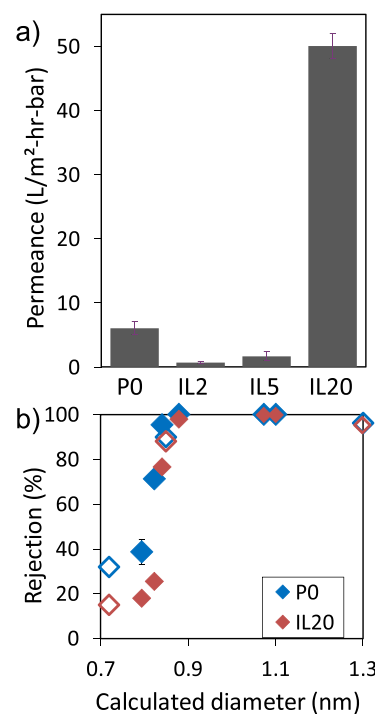


Figure 1. (a) Permeance of zwitterionic copolymer membranes prepared using varying amounts of IL cosolvent. IL20 membranes exhibit permeances 10 times that of P0 membranes. (b) Rejection of membranes prepared with IL20 and P0 solutions. Both membranes show sharp ~1 nm size cutoff with size-based selectivity for charged (solid) and neutral (hollow) solutes.

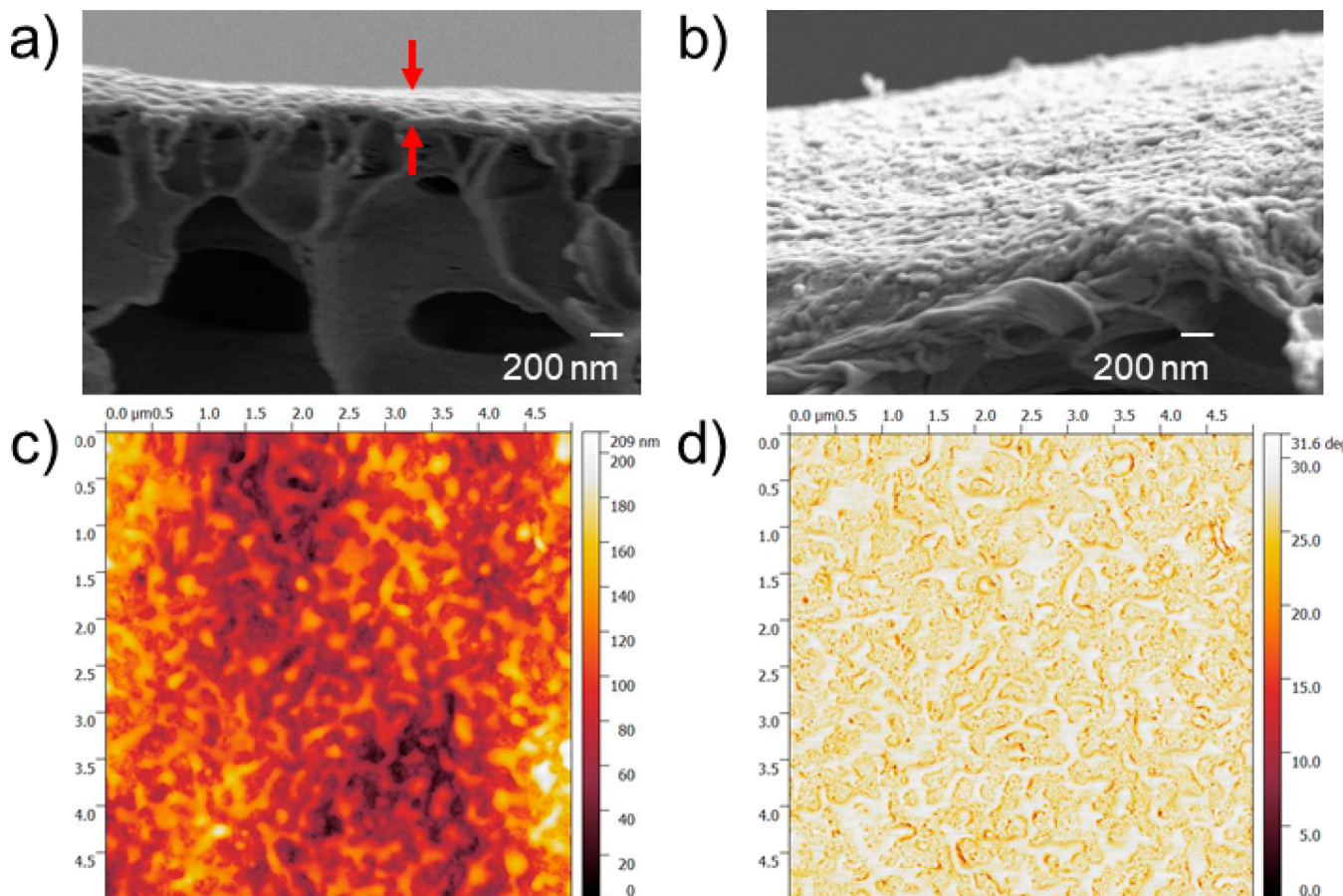


Figure 2. (a) Cross-sectional and (b) tilted FESEM images of IL20 membranes at 50 000 \times magnification, showing <200 nm thick layer with worm-like/nodular features. AFM (c) height and (d) phase images of IL20 membranes show worm-like/nodular features on the surface.

effective pore size. All membranes with and without the IL cosolvent show the same charge-independent size cutoff of \sim 0.8–1 nm when calculated by this method (Figures 1b, S2). Indeed, the pore size distribution in IL20 membranes may be slightly narrower, evidenced by the sharper rejection curve and lower rejection of smaller solutes. We should point out that our method for calculating solute sizes is an underestimate of the hydrodynamic diameter of the solutes, as it does not account for solute geometry or hydration. For instance, the hydrodynamic diameter of vitamin B12 is reported to be around 1.7 nm,³² significantly higher than its calculated diameter of 1.3 nm, implying the true size cutoff is closer to 1.5 nm. However, hydrodynamic diameters for most other solutes used are not easily available. Given the tight rejection curves obtained by this method, this simplified approach for calculating solute size enables prediction of solute rejections by this family of membranes.

This size cutoff corresponds roughly to a nominal MWCO of \sim 1 kDa based on a previous comparison of the P0 membrane with a commercial membrane manufactured by Sartorius (Figure S5).^{11,12} The fact that both charged and uncharged solutes fit onto the same rejection curve implies size-based selectivity, unlike most commercial membranes that exhibit anionic surface charges that lead to enhanced rejection of anionic solutes along with partial salt rejection.^{11,13} This low MWCO is especially promising for bioseparations and textile wastewater treatment.^{13,16} Nominal permeances for 1 kDa MWCO membranes offered by GE, EMD Millipore, and Sartorius range between 1.2 and 7.3 L/m²·h·bar.^{33,34} The

permeance of the RZC membranes described here is approximately seven times that of even the highest value. Furthermore, most of these commercial membranes have charged surfaces. As a result, their selectivity is heavily influenced by solute charge. In contrast, RZCs are overall neutral in charge, so rejection through RZC membranes is size-based. This is evidenced by the fact that charged and uncharged solutes fit onto the same sharp rejection curve (Figure 1b), making separations more predictable.

It is very rare to achieve an order-of-magnitude increase in membrane flux while maintaining and possibly enhancing the selectivity by simply using a cosolvent. To understand what led to this drastic enhancement in performance, we characterized the membrane morphology using high resolution field emission scanning electron microscopy (FESEM). P0 membranes exhibited a \sim 2 μ m thick, dense copolymer coating (Figure S9) on the commercial support (Figure S10). In contrast, FESEM images of the IL20 membrane showed a very thin copolymer coating with interconnected worm-like/cylindrical/nodular features (Figure 2a, b). While it was difficult to clearly identify the separate coating and support layers, the coating thickness was estimated to be <200 nm. The membrane surface was rough, creating a large interfacial area that may further enhance measured water flux. The interconnected features covering the membrane surface were further confirmed by atomic force microscopy (AFM) (Figure 2c, d). The features were 93 ± 19 nm in height. The thickness of the continuous selective layer likely varies and is thinner at the junctions between the nodular features. Bubble point tests

confirmed that no large pores are present on IL20 membranes, indicating a continuous selective layer. This conclusion is also supported by the very small size cutoff consistent with denser selective layers.

On the basis of the morphology of this selective layer, we hypothesized that the RZC may form supramolecular assemblies in some TFE/IL mixtures and that these assemblies deposit onto the porous support and partially merge during the coating process, resulting in the ultrathin, structured selective layers observed. To test this hypothesis, we performed transmission electron microscopy (TEM) on samples prepared by mimicking the membrane making process. A solution containing 0.1 wt % RZC and 0.2 v% IL in TFE, simulating the IL20 solution, was cast on a copper grid (200 mesh, Electron Microscopy Sciences), dipped in isopropanol for 5 min, followed by immersion into water for 5 min, and dried overnight. TEM images of these samples show cylindrical/rod-like structures/nodules 17 \pm 5 nm in diameter that are connected and branched to form interconnected networks (Figure 3). When the same procedure was performed without the IL to simulate P0, no interconnected features were visible (Figure S14).

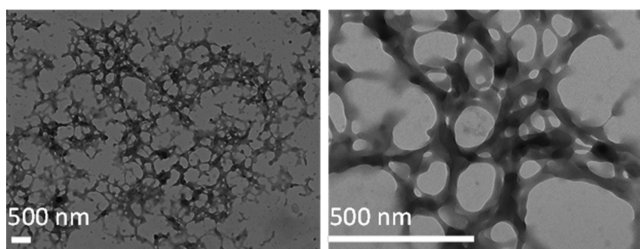


Figure 3. TEM images of samples prepared by mimicking membrane making process with the IL20 solution at 11 000 \times (left) and 49 000 \times (right) magnification. IL20 solutions show an interconnected network of worm-like/cylindrical nodular features. No significant features are observed in the absence of IL.

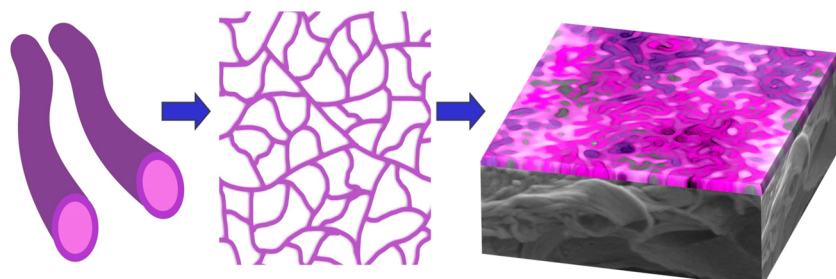
The TEM samples simulate the early stages of the selective layer formation process, due to the more dilute solution that had to be used for preparing TEM samples. The images imply that interconnected networks of rod-like supramolecular assemblies form after the copolymer solution is spread onto the support membrane as TFE evaporates from the thin film. The change in solvent quality leads to the formation of supramolecular assemblies in a particular compositional

window. We hypothesize that these assemblies may be cylindrical or worm-like structures that form an interconnected network (Scheme 1). As these assemblies are larger than the size cutoff of the support membrane, they deposit onto the substrate due to capillary forces. Upon immersion in isopropanol, these structures precipitate out but stay soft, and the assemblies overlap and partially merge. The selective layer is fixed upon immersion into water, a strong nonsolvent. This hypothesis is in agreement with our observation of a thinner membrane selective layer with a nanostructured surface. The lower resistance to flow and high surface area leads to higher permeances.

To better understand the polymer self-assembly in these coating solutions, we performed small-angle X-ray scattering (SAXS) on copolymer/TFE/IL solutions. No identifiable features were observed in the SAXS spectra for coating solutions used to prepare P0, IL2, IL5, and IL20 membranes (Table 1). However, during the membrane manufacturing process, the highly volatile TFE partially evaporates between the coating step and immersion into isopropanol. This step can lead to the creation and organization of supramolecular assemblies as the solvency of the mixture for the zwitterionic and hydrophobic polymer segments changes, leading to the formation of nanostructured membrane selective layers.³⁵ Thus, we prepared four solutions with the same copolymer:IL ratio but simulating the evaporation of 21–45 wt % of TFE, corresponding to copolymer concentrations that increased from 10 to 16.9% (Table S2). Solutions with 13.8 and 12.4% (w/v) (Figure S15) copolymer concentrations indicated the presence of rigid rod-type features, indicated by the linearly increasing asymptote in the Kratky plot (inset). No features were observed for solutions with higher polymer concentrations of 15 and 16.9% (w/v). This implies that the copolymer self-organizes into rod- or worm-like assemblies during the evaporation of TFE after the coating solution is spread onto the support, but this occurs only in a narrow solution composition window. If the coating is immersed into the nonsolvent while the coating solution is within this window, these assemblies can be deposited onto the membrane to form the thin, nodular selective layer observed in the membranes.

These results indicate that solvent evaporation time is a crucial factor in the formation of these supramolecular assemblies. To demonstrate this, we also prepared membranes by spreading the coating solution, air drying for varying durations (20 s to 20 min), followed by immersion into water,

Scheme 1. Growth of Worm-Like/Cylindrical Assemblies during Formation of Zwitterionic Copolymer Membranes Prepared Using IL/TFE Solvent Mixture^a



^aCylinders (left) grow into longer interconnected assemblies (middle) that deposit onto porous substrate and merge to form ultrathin <200 nm thick selective layer. The different colors in the schematic are used for visual clarity and illustration purposes.

which leads to immediate precipitation. Membranes with the shortest drying time of 20 s led to a permeance of 20 L/m²·hr-bar, 4 times the permeance of the P0 membrane. Membranes with longer drying times resulted in thicker coatings and lower permeances but the same selectivity (Figures S16–S18).

In this work, we described the formation of ultrathin, nanostructured RZC selective layers by simply introducing an IL cosolvent, boosting the permeance by up to 10 times with no decline in selectivity. This enabled the manufacture of membranes with ~1000 Da MWCO and permeances as high as 50 L/m²·hr-bar, an exceptionally high flux for this pore size. We found that this increase in membrane permeance occurred for a specific range of coating solution compositions, possibly arising from the self-assembly of the RZCs upon partial evaporation of TFE. This study also provides insights into interactions between ILs and zwitterionic copolymers that may be leveraged for various applications.

ASSOCIATED CONTENT

Supporting Information

The Supporting Information is available free of charge on the ACS Publications website at DOI: [10.1021/acsapm.9b00409](https://doi.org/10.1021/acsapm.9b00409).

Expanded experimental methods and details, additional data on copolymer characterization, membrane selectivity, solute properties, control experiments to account for potential effects of solute adsorption on rejection measurements, solute selectivity of commercial membranes with similar MWCO values, FTIR analysis of membrane selective layers, captive air bubble measurements, membrane morphology, bubble point measurements, TEM analysis, SAXS analysis of polymer solutions, and the effect of drying time on membrane performance ([PDF](#))

AUTHOR INFORMATION

Corresponding Author

*Phone: 617-627-4681; E-mail: ayse.asatekin@tufts.edu.

ORCID

Ilin Sadeghi: [0000-0002-3451-0709](https://orcid.org/0000-0002-3451-0709)

Matthew J. Panzer: [0000-0002-1741-8548](https://orcid.org/0000-0002-1741-8548)

Ayse Asatekin: [0000-0002-4704-1542](https://orcid.org/0000-0002-4704-1542)

Funding

This research was supported by Tufts University; the National Science Foundation (NSF) under Grants CBET-1553661, CBET-1437772, CHE-1508049, and CBET-1802729; and the Massachusetts Clean Energy Center Catalyst Award. TEM was performed utilizing the W.M.Keck foundation Biological Imaging Facility at the Whitehead Institute. The authors thank Dr. Nicki Watson at the Whitehead Institute for help with TEM data acquisition. SAXS was performed at the Center for Materials Science and Engineering X-ray Facility using the Shared Experimental Facilities supported in part by the MRSEC Program of the National Science Foundation under Award DMR 1419807.

Notes

The authors declare the following competing financial interest(s): Ayse Asatekin serves as a Senior Scientific Advisor for ZwitterCo, a start-up that licensed the intellectual property described in this publication. She currently owns no equity and receives no monetary payment from the company.

REFERENCES

- (1) Asatekin, A.; Vannucci, C. Self-Assembled Polymer Nanostructures for Liquid Filtration Membranes: A Review. *Nanosci. Nanotechnol. Lett.* **2015**, *7* (1), 21–32.
- (2) Nunes, S. P.; Behzad, A. R.; Peinemann, K.-V. Self-assembled block copolymer membranes: From basic research to large-scale manufacturing. *J. Mater. Res.* **2013**, *28* (19), 2661–2665.
- (3) Sadeghi, I.; Kaner, P.; Asatekin, A. Controlling and Expanding the Selectivity of Filtration Membranes. *Chem. Mater.* **2018**, *30* (21), 7328–7354.
- (4) Peinemann, K. V.; Abetz, V.; Simon, P. F. Asymmetric superstructure formed in a block copolymer via phase separation. *Nat. Mater.* **2007**, *6* (12), 992–6.
- (5) Nunes, S. P. Block Copolymer Membranes for Aqueous Solution Applications. *Macromolecules* **2016**, *49* (8), 2905–2916.
- (6) Phillip, W. A.; Dorin, R. M.; Werner, J.; Hoek, E. M. V.; Wiesner, U.; Elimelech, M. Tuning Structure and Properties of Graded Triblock Terpolymer-Based Mesoporous and Hybrid Films. *Nano Lett.* **2011**, *11* (7), 2892–2900.
- (7) Phillip, W. A.; Hillmyer, M. A.; Cussler, E. L. Cylinder Orientation Mechanism in Block Copolymer Thin Films Upon Solvent Evaporation. *Macromolecules* **2010**, *43* (18), 7763–7770.
- (8) Clodt, J. I.; Bajer, B.; Buhr, K.; Hahn, J.; Filiz, V.; Abetz, V. Performance study of isoporous membranes with tailored pore sizes. *J. Membr. Sci.* **2015**, *495*, 334–340.
- (9) Sadeghi, I.; Kronenberg, J.; Asatekin, A. Selective Transport through Membranes with Charged Nanochannels Formed by Scalable Self-Assembly of Random Copolymer Micelles. *ACS Nano* **2018**, *12* (1), 95–108.
- (10) Qu, S.; Dilenschneider, T.; Phillip, W. A. Preparation of chemically-tailored copolymer membranes with tunable ion transport properties. *ACS Appl. Mater. Interfaces* **2015**, *7*, 19746–19754.
- (11) Bengani, P.; Kou, Y.; Asatekin, A. Zwitterionic copolymer self-assembly for fouling resistant, high flux membranes with size-based small molecule selectivity. *J. Membr. Sci.* **2015**, *493*, 755–765.
- (12) Bengani-Lutz, P.; Converse, E.; Cebe, P.; Asatekin, A. Self-Assembling Zwitterionic Copolymers as Membrane Selective Layers with Excellent Fouling Resistance: Effect of Zwitterion Chemistry. *ACS Appl. Mater. Interfaces* **2017**, *9* (24), 20859–20872.
- (13) Bengani-Lutz, P.; Zaf, R. D.; Culfaç-Emecen, P. Z.; Asatekin, A. Extremely fouling resistant zwitterionic copolymer membranes with ~1nm pore size for treating municipal, oily and textile wastewater streams. *J. Membr. Sci.* **2017**, *543*, 184–194.
- (14) Bredas, J. L.; Chance, R. R.; Silbey, R. Head Head Interactions in Zwitterionic Associating Polymers. *Macromolecules* **1988**, *21* (6), 1633–1639.
- (15) Wu, T. Y.; Beyer, F. L.; Brown, R. H.; Moore, R. B.; Long, T. E. Influence of Zwitterions on Thermomechanical Properties and Morphology of Acrylic Copolymers: Implications for Electroactive Applications. *Macromolecules* **2011**, *44* (20), 8056–8063.
- (16) Tunc, M. S.; Yilmaz, L.; Yetis, U.; Culfaç-Emecen, P. Z. Purification and Concentration of Caustic Mercerization Wastewater by Membrane Processes and Evaporation for Reuse. *Sep. Sci. Technol.* **2014**, *49* (13), 1968–1977.
- (17) Petersen, R. J. Composite Reverse Osmosis and Nanofiltration Membranes. *J. Membr. Sci.* **1993**, *83* (1), 81–150.
- (18) Behera, K.; Pandey, S. Ionic liquid induced changes in the properties of aqueous zwitterionic surfactant solution. *Langmuir* **2008**, *24*, 6462–6469.
- (19) Hoffmann, H.; Rauscher, A.; Gradzielski, M.; Schulz, S. F. Influence of ionic surfactants on the viscoelastic properties of zwitterionic surfactant solutions. *Langmuir* **1992**, *8*, 2140–2146.
- (20) Tung, S.-H.; Huang, Y.-E.; Raghavan, S. R. A new reverse wormlike micellar system: mixtures of bile salt and lecithin in organic liquids. *J. Am. Chem. Soc.* **2006**, *128*, 5751–5756.
- (21) Zhao, J.; Chai, Y. D.; Zhang, J.; Huang, P. F.; Nakashima, K.; Gong, Y. K. Long circulating micelles of an amphiphilic random copolymer bearing cell outer membrane phosphorylcholine zwitterions. *Acta Biomater.* **2015**, *16*, 94–102.

(22) Marsh, K. N.; Boxall, J. A.; Lichtenhaller, R. Room temperature ionic liquids and their mixtures—a review. *Fluid Phase Equilib.* **2004**, *219* (1), 93–98.

(23) Yi, Z.; Zhu, L.-P.; Zhang, H.; Zhu, B.-K.; Xu, Y.-Y. Ionic liquids as co-solvents for zwitterionic copolymers and the preparation of poly(vinylidene fluoride) blend membranes with dominated β -phase crystals. *Polymer* **2014**, *55* (11), 2688–2696.

(24) Rao, V. G.; Ghatak, C.; Ghosh, S.; Mandal, S.; Sarkar, N. The chameleon-like nature of zwitterionic micelles: the effect of ionic liquid addition on the properties of aqueous sulfobetaine micelles. *ChemPhysChem* **2012**, *13* (7), 1893–901.

(25) Lind, F.; Rebollar, L.; Bengani-Lutz, P.; Asatekin, A.; Panzer, M. J. Zwitterion-Containing Ionogel Electrolytes. *Chem. Mater.* **2016**, *28* (23), 8480–8483.

(26) Brown, R. H.; Duncan, A. J.; Choi, J.-H.; Park, J. K.; Wu, T.; Leo, D. J.; Winey, K. I.; Moore, R. B.; Long, T. E. Effect of Ionic Liquid on Mechanical Properties and Morphology of Zwitterionic Copolymer Membranes. *Macromolecules* **2010**, *43* (2), 790–796.

(27) Maddikeri, R. R.; Colak, S.; Gido, S. P.; Tew, G. N. Zwitterionic Polymersomes in an Ionic Liquid: Room Temperature TEM Characterization. *Biomacromolecules* **2011**, *12* (10), 3412–3417.

(28) Zhao, M.; Gao, Y.; Zheng, L. Liquid Crystalline Phases of the Amphiphilic Ionic Liquid N-Hexadecyl-N-methylpyrrolidinium Bro-mide Formed in the Ionic Liquid Ethylammonium Nitrate and in Water. *J. Phys. Chem. B* **2010**, *114*, 11382–11389.

(29) Asatekin, A.; Menniti, A.; Kang, S. T.; Elimelech, M.; Morgenroth, E.; Mayes, A. M. Antifouling nanofiltration membranes for membrane bioreactors from self-assembling graft copolymers. *J. Membr. Sci.* **2006**, *285* (1–2), 81–89.

(30) Asatekin, A.; Olivetti, E. A.; Mayes, A. M. Fouling resistant, high flux nanofiltration membranes from polyacrylonitrile-graft-poly(ethylene oxide). *J. Membr. Sci.* **2009**, *332* (1–2), 6–12.

(31) Asatekin, A.; Mayes, A. M. Responsive Pore Size Properties of Composite NF Membranes Based on PVDF Graft Copolymers. *Sep. Sci. Technol.* **2009**, *44* (14), 3330–3345.

(32) Amsden, B. Solute Diffusion within Hydrogels. Mechanisms and Models. *Macromolecules* **1998**, *31* (23), 8382–8395.

(33) Flat sheet membranes specification sheet. <https://www.sterlitech.com/flat-sheet-membranes.html> (accessed April 30, 2019).

(34) EMD Millipore UF Membranes Data Sheet. <https://www.lenntech.com/Data-sheets/Millipore-Ultrafiltration-Membranes-L.pdf> (accessed April 30, 2019).

(35) Marques, D. S.; Vainio, U.; Chaparro, N. M.; Calo, V. M.; Bezahd, A. R.; Pitera, J. W.; Peinemann, K. V.; Nunes, S. P. Self-assembly in casting solutions of block copolymer membranes. *Soft Matter* **2013**, *9* (23), 5557–5564.